JASS Journal of Astronomy and Space Sciences

X-ray Data Analysis to Search for Magnetar Candidates in the Galactic Plane

Woochan Park, Hongjun An[†]

Department of Astronomy and Space Science, Chungbuk National University, Cheongju 28644, Korea

We report on our Galactic plane searches for magnetars in the archival *Chandra* X-ray Observatory (CXO) data. We summarize the properties of known magnetars and use them to establish a procedure for magnetar searches. The procedure includes four steps: source finding, spectral characterization, optical counterpart checks, and period searches. We searched 1,282 archival CXO observations, found 32,838 X-ray sources, and selected 25 intriguing candidates using the developed procedure. Although we do not firmly identify a magnetar among them, we significantly reduced the number of targets in future magnetar searches to be done with better X-ray telescopes.

Keywords: magnetar, *Chandra*, X-ray telescopes

1. INTRODUCTION

Magnetars are isolated neutron stars powered by strong magnetic fields that are typically greater than 10^{14} G (Thompson & Duncan 1995) and which emit radiation almost exclusively in the X-ray band. The X-ray emission spectra of magnetars have two main components: thermal emission from the surface and non-thermal radiation in the magnetosphere. Although some magnetars are detected in the optical or infrared band, they are very faint with a magnitude greater than 20. Similar to typical pulsars, magnetars turn with a rotation period (P), and the first derivative ($\dot{P}$) in the range of P = 2 – 12 sec and $\dot{P} = 10^{-13}$–10^{-10} sec sec^{-1}. In addition, magnetars often exhibit strong X-ray activities that include brightening in the forms of short bursts, outbursts, and giant flares. These transient behaviors last from milliseconds to years (see Rea et al. 2010; Olausen & Kaspi 2014; Mereghetti et al. 2015 for review).

The first magnetar was discovered in 1979 through the detection of repeated bursts from the direction of the Large Magellanic Cloud (LMC; Mazets et al. 1979). The bursts had softer spectra than those of gamma-ray bursts (GRBs), and hence, the source was initially called a "soft gamma repeater (SGR)". Subsequently, the 7 sec X-ray pulsar 1E 2259+586 was discovered in the galactic supernova remnant CTB 109 (Fahlman & Gregory 1981). This pulsar was unusual in that its X-ray luminosity was larger than the rotation power without any signature of accretion. Therefore, it was initially called an "anomalous X-ray pulsar (AXP)". Subsequently, more SGRs and AXPs were discovered and were thought to be different types of neutron stars. However, Thompson & Duncan (1995) theoretically unified them using a magnetar model, and Gavriil et al. (2002) indeed discovered SGR-like bursts from an AXP (1E 1048.1-5937) subsequently. Hence, the distinction between SGRs and AXPs is blurred observationally as well as theoretically.

A magnetar can be firmly identified only by measuring the spin-inferred magnetic field strength B = $3.2 \times 10^{19} \sqrt{P\dot{P}}$ G (>10^{14} G). Historically, the majority of the known magnetars were discovered during their X-ray bursts/outbursts via a targeted search for periodicity when the source was bright. The sensitivity of X-ray observatories has improved significantly, and it may now be possible to discover a relatively faint magnetar serendipitously, even if the magnetar is not in the outburst state. Indeed, several quiescent magnetars have been discovered in this manner

(e.g., J164710.2-455216; Muno et al. 2006). Of course, the determination of the magnetic field strength is the most crucial test, but it should be noted that some magnetars are known to have lower magnetic fields (e.g., Rea et al. 2013) than a conventional rotation-powered pulsar (e.g., PSR B1509-58; Wang et al. 2013; Chen et al. 2016). Therefore, we cannot identify a magnetar based on the magnetic field alone. The X-ray spectra of conventional X-ray bright rotation-powered pulsars (e.g., weak or no blackbody emission) differ significantly from those of magnetars, and thus, careful characterization of the spectrum is required.

Finding more magnetars is important for many reasons. The origin and evolution of magnetars, and their relation to other neutron stars are not yet well understood, and thus, population studies with larger samples of magnetars are required. In addition, magnetars are promising targets of future gravitational wave detectors because their strong internal magnetic stress may deform the star (Beloborodov & Li 2016), and such deformed rotating stars emit gravitational waves (Bonazzola & Gourgoulhon 1996).

Although this deformation is estimated to be too small for near-future gravitational detectors to detect their waves, these may be detected as stochastic background or as a point source if the distortion is very large, perhaps during a giant flare period.

In this study, we searched for magnetars among X-ray point sources in the Chandra archival data using a procedure we developed. In Section 2, we report the results of our study in terms of the properties of known magnetars; these properties were used to develop a procedure and automated packages for selecting magnetar candidates. We present the procedure and apply it to archival Chandra data in Section 3 and present our conclusions in Section 4.

2. BASIC PROPERTIES OF KNOWN MAGNETARS

To select potential magnetar candidates for further identification, we need to know the properties of magnetars. This was achieved through a statistical study of known magnetars. The spatial, spectral, and temporal properties of known magnetars are well summarized in the magnetar catalog and in the study by Olausen & Kaspi (2014). We used this catalog and reference to gain a quantitative understanding of magnetar properties and then make our selections. It should be noted that 29 magnetars are listed in the catalog; however, we needed to know their spectral/temporal properties very well to use them to find similar X-ray sources. Therefore, we used the information from only 19 magnetars (from among

the 29 listed) of which the spectral and temporal properties were well characterized.

The *Chandra* database is immense, and we needed to select regions of the sky wherein magnetars were likely to be found. This could be done based on the work of Olausen & Kaspi (2014). They found that magnetars are rather randomly distributed in galactic longitude and lie within 5° from the galactic plane (Figs. 3 and 4; Olausen & Kaspi 2014). Therefore, we used observations made in this region.

The X-ray spectra of magnetars are generally described by a blackbody-plus-power-law (BBPL) model, although the emissions of some magnetars appear to be a simple power law (PL) or a simple blackbody (BB), perhaps because of limited statistics. In some magnetars, strong hard X-ray emissions of >10 keV are observed (Kuiper et al. 2006) and a putative detection of gamma rays was made from a magnetar (e.g., Wu et al. 2013). The latter, if real, will aid in determining the emission geometry (e.g., Harding 2013) and can be compared with various emission scenarios (e.g., An et al. 2015); these properties were not used in our identification procedure because we are using soft X-ray band data (<10 keV). To characterize the general spectral properties, we obtained the spectral parameters from the magnetar catalog and generated distributions of BB temperature (kT) and PL photon index (Γ). Fig. 1 shows the kT and Γ distributions of 12 magnetars with BBPL spectra. For these magnetars, the BB temperature is rather tightly bound (0.36 - 0.58 keV) and the photon index is in the range of 1.6 - 4. We used these ranges for the spectral searches below. The other seven magnetars exhibited a single-component spectrum (BB or PL) for which kT and Γ were in the ranges of 0.12 - 0.5 keV and 1 - 3.45, respectively.

The temporal properties of magnetars are crucial for the final confirmation that an X-ray source is a magnetar, and these should be determined by measuring pulsations (periodic modulation). The general temporal properties of the 19 best-known magnetars are shown in Fig. 2. However, it was unlikely that we would detect pulsations in our study given the limited statistics and temporal baseline. This is because, for the detection of pulsations, the time resolution of the observatory is required to be sufficiently good and the pulsation should be strong. The time resolution for the *Chandra* X-ray Observatory (CXO) data we used (image mode) is 3.24 sec (full frame, most of the observations) or 0.4 sec (sub-array); thus, at best, sources with a period greater than ~6 sec or 0.8 sec could be detected as pulsating sources. Furthermore, for the typical number of photons collected (~100 photons per source), the pulsed fraction of the potential magnetar should be greater than 30 % for its pulsations to be detected. Among the 19 best-known magnetars, 11 had a
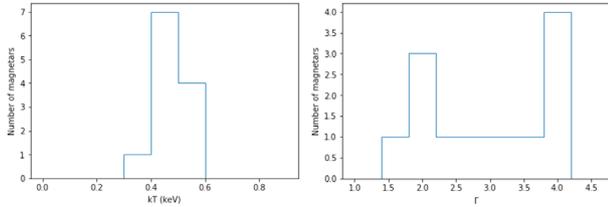
Fig. 1. Distribution of blackbody temperatures and photon indices of known magnetars with spectra that fit the blackbody-plus-power-law model: (left) blackbody temperature (kT); (right) photon index (Γ).
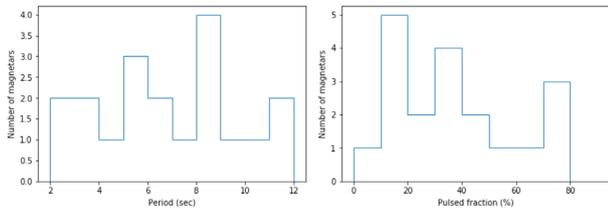
Fig. 2. Temporal properties of the 19 best-known magnetars: (left) period distribution; (right) distribution for pulsed fraction. The pulsed fractions were obtained from the literature (Gotthelf et al. 2004; Campana et al. 2007; Esposito et al. 2007; Israel et al. 2007; Rea et al. 2007; Tam et al. 2008; Tiengo et al. 2008; Zhu et al. 2008; Esposito et al. 2009; Tiengo et al. 2009; Halpern & Gotthelf, 2010b; Bernardini et al. 2011; Rea et al. 2012; An et al. 2013; Rea et al. 2013; An et al. 2014; Camero et al. 2014; Israel et al. 2016; Camilo et al. 2018).

period >6 sec and 11 had a pulsed fraction >30 % (see Fig. 2). This implies that the probability that we would detect the pulsations of a source (if it was a magnetar) is only ~33 %. Because the detection of pulsations would almost certainly identify the source (no longer a candidate), we retained such sources in the candidate list even if we did not detect pulsations from them.

3. OBSERVATIONAL DATA ANALYSIS AND RESULTS

We used the archival data of observations made by CXO between January 2002 and January 2018. The observations were performed with an advanced charge-couple device (CCD) imaging spectrometer (ACIS). The ACIS-I detector consists of six CCDs and provides high-resolution imaging over a ~17' field of view (FOV). The angular resolution is very good with a half-power diameter less than 0.5'', and the time resolution is ~3.2 sec (Garmire et al. 2003). By using a restricted region of the detector, a better time resolution (0.4 sec) can be achieved with the reduction of the FOV. While there are other X-ray observatories (*Swift*, *XMM-Newton*, etc.), their angular resolution is not sufficient for this study. Therefore, we only use *Chandra* data for this study.

We used 1,282 *Chandra* observations (the typical exposure per observation is 20 ks) downloaded from the High Energy

Astrophysics Science Archive Research Center data arch-ive (https://heasarc.gsfc.nasa.gov/cgi-bin/W3Browse/w3browse.pl). These data were reprocessed with the Chandra_repro tool of CIAO (*Chandra* Interactive Analysis of Observations) 4.9 along with CALDB 4.7.6, and we analyzed the data following a procedure we developed, which is described below.

3.1 Magnetar Search Procedure and Data Analysis

Based on the general properties of the best-known mag-netars (Section 2), we developed the following procedure for magnetar searches:

① We found point sources in the *Chandra* image. We selected point sources because magnetars are isolated neutron stars. Although we could have used the existing Chandra catalog (Evans et al. 2010) directly, we chose to reanalyze the data for a more accurate determination of the spectral parameters required in other steps (customized spectral models in step ②) and the position of each X-ray source in step ③. Because the number of detected events from a source is required to be sufficiently large for spectral characterization, we ignored sources with <30 detected events.

② For the point sources found in step ①, we fitted the spectra using a BB, PL, and BBPL model to measure the spectral parameters. We then selected sources with a BB temperature (kT) in the range 0.36 - 0.58 keV and PL photon index (Γ) in the range of 1.6 - 4 for the BBPL. These are typical magnetar emissions (Section 2). In addition, we separately collected sources with kT in the range of 0.12 - 0.5 keV for BB emission or Γ in the range of 1.0 - 3.45 for PL emission.

③ We searched optical and infrared (IR) catalogs for bright optical sources near the X-ray sources. It was required that there be no bright optical source within a specified error circle for each source. The size of the error circle was determined by the uncertainty of the source position (step ①) and of the CXO absolute astrometry (~1" at 99 % confidence). These two uncertainties were added in quadrature. This was to ensure that the X-ray source had no bright optical counterpart with 3σ confidence because magnetars are very faint in the optical/IR band (>20 mag). For this, we used the NOMAD and 2MASS catalogs (Zacharias et al. 2004; Skrutskie et al. 2006). It should be noted that the position uncertainties in these catalogs are negligible as compared to the CXO uncertainties.

④ We performed a timing analysis to detect pulsation. Detection of pulsation would be strong evidence that the X-ray source is a magnetar, although a final confirmation

would need to be obtained by measuring the period derivative (i.e., magnetic field strength). In addition, long-term variability (e.g., outburst tail) may aid in identifying a candidate, but in general, the fields are not observed multiple times. Therefore, we do not consider this here.

For reference, we applied this procedure to the known magnetars in the catalog to estimate the probability of discovering a magnetar if there was a real magnetar in the field. Four of the 19 magnetars passed all four steps, and thus, the obtained probability was 21 %. If we assume that the spectral/temporal properties of magnetars are all independent, the probability would be 16 % (14/19 for step ①, 12/19 for step ②, 19/19 for step ③, and 11/19 × 11/19 for step ④).

Data analysis was performed for each of the steps in the following manner. For step ①, we used the "wavedetect" tool of CIAO, which finds X-ray sources based on a wavelet decomposition technique and reports the best position and uncertainty. For each of these sources, we extracted events in the 0.5 – 10 keV band within a circular region with a radius of 3'' centered at the source position for the source spectrum, and an annular region with an inner radius of 3'' and an outer radius of 5'' for the background spectrum. Spectral response files were generated separately for each source using the "specextract" tool of CIAO, and each spectrum was fitted using the BBPL, PL, and BB models in XSPEC[3]. We used the tbabs photoelectric absorption model in XSPEC with the abundance table of Anders & Grevesse (1989) and photoelectric cross-sections from Verner et al. (1996). We note that it is optimal to use an elliptical region to maximize the signal-to-noise ratio for off-axis sources, but 3'' is sufficiently large for the majority of the sources we find (at off-axis angles <6').

For the sources that passed the spectral test, we checked for optical or IR counterparts using the NOMAD and 2MASS catalogs. We searched for nearby optical sources in the catalogs and calculated the angular separation $|\vec{\Delta\theta}| = |\vec{\theta}_s - \vec{\theta}_c|$ between the X-ray and optical sources, where $\vec{\theta}_s$ and $\vec{\theta}_c$ are the positions of the X-ray and optical/IR sources. The uncertainty of the separation was calculated by summing the individual uncertainties in quadrature $|\vec{d\theta}| = \sqrt{|\vec{\delta\theta_s^2}| + |\vec{\delta\theta_c^2}|}$, where $\vec{d\theta_s}$ and $\vec{d\theta_c}$ are the position uncertainties for the X-ray and optical/IR sources). Because *Chandra* images have an absolute astrometry uncertainty of 1'' (3σ), we added this to the position uncertainties in quadrature ($|\vec{d\theta_E}| = \sqrt{|\vec{d\theta^2}| + |\vec{d\theta_a^2}|}$, where $\vec{d\theta_a}$ is the *Chandra* absolute astrometric accuracy). The significance for coincidence K_s was then calculated using $K_s = |\vec{\Delta\theta}| / |\vec{d\theta_E}|$, and we selected X-ray sources with $K_s > 3$ for any nearby optical/IR sources.

Finally, we performed a timing analysis for the sources that passed steps ①–③ using the Z^2_1 test (Buccheri et al. 1983) to find any periodic modulation. Because of the limited time resolution, we tested for periodicity in the range of 5 - 15 sec (for observations with a 3.24 sec time resolution) or 0.8 - 15 sec (for observations with a 0.4 sec time resolution). We scanned this range with the time-step $\Delta T=10^{-7}$ and then calculated the Z^2_1 value for each test period. The Z^2_1 test is particularly useful because the distribution function is known; Z^2_1 values are known to follow the χ^2 statistic with two degrees of freedom. The larger Z^2_1 is, the more likely that the source is pulsating. We calculated the significance for the maximum Z^2_1 in the scan range for each source while correcting for the trial factor.

Because the data set we were analyzing was very large and included several X-ray sources, we created a python package to automate the analysis procedure. Each step of the procedure (in Section 3.1) was implemented in the package, and after each step, the obtained intermediate results were recorded in a file.

3.2 Verification of the Procedure and Analysis Results

3.2.1 Verification of the Procedure with a Known Magnetar

After setting up the search procedure, we verified it using a known magnetar. We analyzed a 40 ks Chandra observation (Obs. ID 5411) that has the magnetar CXOU J164710.2-455216 (J1647 hereafter) in its field. We first searched for X-ray sources in the observation using the "wavedetect" tool and found J1647 (Fig. 3 top left). The best source position was R.A. = 16^h 47^m 10.199^s, Decl. = −45° 52′ 17.33′′ with a position uncertainty of 1′′, which is consistent with the catalog values (R.A. = 16^h 47^m 10.2^s, Decl. = −45° 52′ 16.9′′). The source spectra were fitted with a BB (kT=0.49 keV), a PL (Γ=3.28), and a BBPL model (kT=0.53 keV, Γ=3.3). The best-fit spectral parameters were well within the range we set for magnetar candidates in Section 3.1 (step ②). Next, we confirmed that this magnetar had no bright optical or IR counterpart (Fig. 3 bottom left) and that the source was pulsating (Fig. 3 bottom right). As expected, we identified this magnetar as a good magnetar candidate using the procedure and the analysis package we developed, thereby verifying them.

3.2.2 Blind Tests with Known Magnetars in the Field

The field we studied was very large and had within it six known magnetars (1E 1547.0-5408, CXOU J171405.7-381031, SGR J1745-2900, SGR 1806-20, SGR 1833-0832, and SGR
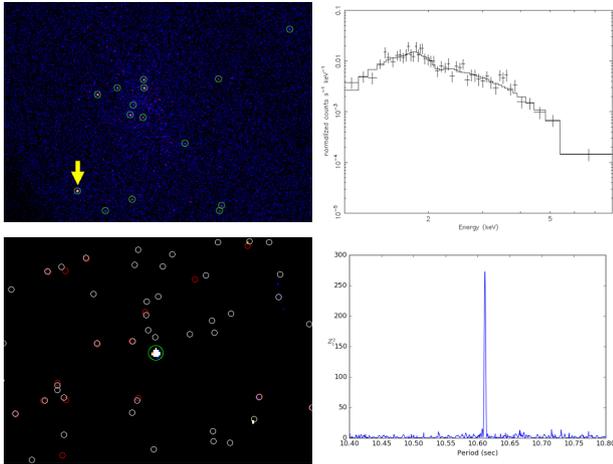
Fig. 3. Analysis results of the data obtained for the magnetar CXOU J164710.2-455216. We applied the four-step procedure we developed to "find" this magnetar. As expected, the magnetar passed all four steps. Top left: Green circles represent X-ray sources detected in the image analysis, and the yellow arrow denotes J1647. Top right: X-ray spectrum of J1647 in the 0.5 – 10 keV band. The best-fit blackbody-plus-power-law model is also shown (solid line). Bottom left: Result of a counterpart search. White circles indicate optical sources in the NOMAD catalog and red circles indicate infrared sources in the 2MASS catalog. Bottom right: Results of timing analysis. Clear pulsations are observed at the period of J1647 (P = 10.6108 sec).

Table 1. Results obtained on applying the new procedure to six magnetars in our search field, where "O" indicates "pass"

Name	Source finding	Spectrum	Counter-parts	Timing
1E 1547.0-5408	O: 274 counts	O: BBPL	O	X: 2.07 sec
CXOU J 171405-381031	O: 1,197 counts	O: BBPL	O	X: 3.82 sec
SGR J1745-2900	O: 1,902 counts	O: BBPL	O	X: 3.76 sec
SGR 1806-20	O: 3,137 counts	O: BBPL	O	X: 7.54 sec
SGR 1833-0832	O: 3,323 counts	O: BBPL	O	O: 7.56 sec
SGR 1900+14	O: 6,044 counts	O: BBPL	O	X: 5.19 sec

1900+14). All these were found in the new imaging analysis. The X-ray spectra of these magnetars fit well with the BBPL model. None of them had an optical or IR counterpart. Hence, these magnetars would have become candidates even if they were not already known to be magnetars (Table 1).

In the subsequent timing analysis, the pulsation of SGR 1833-0832 was detected with a spin period of 7.5654 sec, which was consistent with that measured by Esposito et al. (2011). Thus, we could identify this one as an "almost-certain" magnetar, thereby again verifying the procedure and packages, as in the case of J1647. However, the pulsation of the other magnetars was not detected. This was owing to the short period or perhaps to the small pulsed fraction (Mereghetti et al. 2006; Sato et al. 2010; Dib et al. 2012; Kaspi et al. 2014). For example, SGR 1806-20 is very bright but has a very small pulsed fraction (~2.5 %; Woods et al.

2007). The pulsed fraction is further reduced when blurred owing to the *Chandra* time resolution of 3.24 sec. Hence, the pulsation of SGR 1806-20 was not detected despite having many collected events. In Table 1, we summarize the results of each step for six magnetars.

3.2.3 Search for Magnetar Candidates

After all the known magnetars in the field were studied, we inspected other sources. In our image analysis, we found 32,838 point sources with known positions. We fitted the spectrum of each of the sources with a BBPL, a BB, and a PL model and found that 149 (BBPL), 3,109 (BB), and 10,744 (PL) sources, respectively, passed step ②. In Fig. 4 (left), we present the best-fit kT and Γ for 135 sources with spectra that are fitted to the BBPL model. The results for single-component models (a PL or a BB) are shown in Fig. 4 (middle and right). It should be noted that some sources are in multiple spectral categories. Next, we checked if the X-ray sources have an optical/IR counterpart and eliminated those with a counterpart. This left 25 (BBPL), 811 (BB), and 1,725 (PL) X-ray sources. The analysis results are summarized in Table 2.

Finally, we performed a timing analysis. The maximum Z_1^2 value for the sources that passed steps ①–③ was 31.54, which corresponded to the null hypothesis probability of 1.41×10^{-7}. This is small; however, considering the trial factor of 10^8, this is not significant. In conclusion, we did not find significant pulsations in any of the sources.

Theoretically, the spectrum of a magnetar should be modeled using a BBPL model (Beloborodov 2013), and indeed, the majority of magnetars have a two-component emission. Therefore, we might find better candidates by investigating the 25 sources with a two-component emission. We list these separately in Table 3. In this table, we also report the best-fit parameters with the uncertainty. The parameters were not very well constrained for these faint sources. For very faint sources, some parameters were not constrained. In this case, we maintained those parameters fixed to derive uncertainties for the other parameters. Because some of the sources might already have been studied, we searched the SIMBAD catalog (https://simbad.u-strasbg.fr/simbad) to check if any of the sources had been previously identified. We found that XMMU J173203.3-344518 (hereafter, J1732) in the table was previously identified as a potential pulsar in a supernova remnant (Halpern & Gotthelf 2010a). There are some other sources listed in the CXO or *XMM* catalog, but their nature is not yet clear.
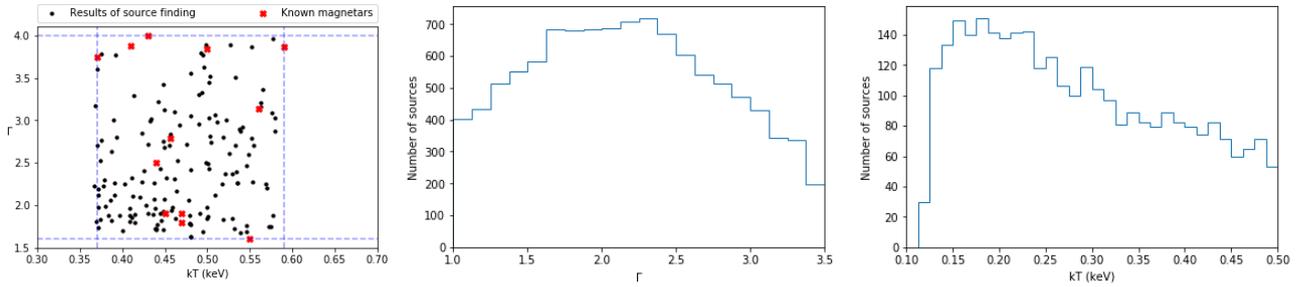
Fig. 4. Spectral parameters for X-ray sources that pass step ②: (left) kT-Γ diagram. Black dots indicate X-ray sources fitted to the blackbody-plus-power-law model, and red squares indicate known magnetars. Middle: Γ distribution for sources with spectra that are fitted to a single power-law model. (Right) kT distribution for sources with spectra that are fitted to a single blackbody model.

Table 2. Number of X-ray sources that passed each step of our procedure for three spectral-model categories

Actions	Blackbody + Power-law	Blackbody	Power-law
Source finding	32,838	32,838	32,838
Spectral analysis	149	3,109	10,744
Counterpart search	25	811	1,725
Timing analysis	0	0	0

Table 3. Position and spectral properties of 25 sources that fit a blackbody-plus-power-law model

Obs. ID	N_H[a]	kT[b]	Γ[c]	F_{BB}[d]	F_{PL}[e]	R.A.	Dec
17849	1.00E-04	0.5(2)	1.6	0.0203(6)	0.02	283.2896(3)	-8.6410(3)
6420	1.1(5)	0.58(8)	1.9	0.0145(6)	0.002	275.1163(3)	-16.1805(3)
6420	1.9(4)	0.37	2.5(4)	0.03	0.21(1)	275.1217(3)	-16.1774(3)
6421	1.2(3)	0.48(9)	1.8(8)	0.23(6)	0.6(1)	275.1243(3)	-16.1780(3)
972	1.5(5)	0.4(1)	1.7	0.022(3)	0.014	275.0913(3)	-16.1849(3)
972	1.1(2)	0.43(8)	1.9(5)	0.22(3)	0.63(6)	275.1243(3)	-16.1781(3)
8898	1.1(3)	0.54	1.7(5)	0.02	0.050(2)	344.0925(3)	62.0335(3)
14366	1.00E-04	0.53	2.4(5)	0.004	0.0080(3)	87.9971(3)	32.4984(3)
2556	1.4(2)	0.57	2.2(2)	0.06	0.255(4)	134.7727(3)	-47.5090(3)
3501	0.50(6)	0.44(4)	2.26	0.1079(9)	0.16	156.0059(3)	-57.7582(3)
4495	1.00E-04	0.54	2.3(3)	0.005	0.0127(2)	160.9904(3)	-59.5430(3)
6371	2.2(5)	0.38	1.8(7)	0.09	0.13(1)	125.7350(3)	-42.6798(3)
6433	1.36(2)	0.43	2.7(3)	0.006	0.150(6)	134.8650(3)	-43.7555(3)
12330	0.6(3)	0.45	2.7(8)	0.008	0.041(8)	168.7830(3)	-61.2585(3)
13787	0.4(2)	0.47	2.5(5)	0.006	0.045(2)	165.4606(3)	-60.9758(3)
16007	1.0(2)	0.52	1.8(2)	0.02	0.127(1)	165.4422(3)	-61.0242(3)
16007	1.2(1)	0.42	2.1(2)	0.03	0.177(2)	165.4436(3)	-61.0236(3)
2314	2.4(1)	0.47(2)	3.1	30.9(3)	60.5	244.4009(3)	-51.0402(3)
2315	2.65(7)	0.50(4)	3.9	14.9(3)	205	244.4008(3)	-51.0402(3)
2316	2.0(1)	0.50(2)	2.8	27.7(1)	21.5	244.4009(3)	-51.0401(3)
3514	2.3(1)	0.45(4)	3.4	8.5(2)	39	244.4009(3)	-51.0402(3)
3517	1.6(1)	0.50(3)	3.1	6.7(1)	8.7	244.4010(3)	-51.0402(3)
4477	0.9(1)	0.53	3.9(2)	0.06	1.9(1)	261.1860(3)	-34.2013(3)
5592	1.4(2)	0.45(4)	1.9	5.2(1)	2.5	244.4010(3)	-51.0402(3)
9139	1.7(2)	0.45(2)	1.8(5)	4.70(1)	2.5(2)	263.0142(3)	-34.7547(3)

Note. 1-σ uncertainties are shown in parenthesis. Parameters without an uncertainty are held fixed.
[a] Hydrogen column density in units of 10^{22} cm^{-2}
[b] Blackbody temperature
[c] Power-law photon index
[d] Blackbody flux in units of 10^{-12} erg cm^{-2} sec^{-1} in the 0.5 – 10 keV band
[e] Power-law flux in units of 10^{-12} erg cm^{-2} sec^{-1} in the 0.5 – 10 keV band

4. DISCUSSION AND CONCLUSIONS

We developed a new procedure to search for magnetar candidates. The procedure was implemented in a python package that could analyze a large data set automatically. The package can be used to reduce the number of targets (good magnetar candidates) in more detailed searches of current and future X-ray satellite data. We used the package to analyze 1,282 *Chandra* observations and selected 25, 811, and 1,725 magnetar candidates, using a BBPL, BB, and PL spectrum, respectively. Unfortunately, pulsation was not found in the case of any of the sources.

We verified the procedure and software package using a known magnetar: J1647 was confirmed using the new procedure. In addition, we identified one among six previously known magnetars in our survey field. This implies a detection probability of 10 - 47 % (68 % confidence range between 16 % and 84 % percentiles) assuming a Poisson distribution. This detection probability is consistent with those (21 % or 16 %; see Section 3.1) we estimated using the 19 best-known magnetars. This reconfirmed that the procedure and software package work properly.

We did not identify pulsation in the case of any of the sources. Should there have been a real magnetar in the list (Table 3), there is a 16 % probability that we would have discovered it. With this probability, we can estimate the number of potential magnetars in the survey; as no magnetar was discovered using our method, we infer that there are less than 14 magnetars amongst the considered candidates with 90 % confidence. That is, if there were more than 14 magnetars in our survey, there is a 90 % chance we would have discovered one (or more).

With respect to the 25 sources with BBPL emission (Table 3), it is likely that not all of them would be magnetars. Some of them would be isolated pulsars, low-mass pulsar binaries, or pulsars in pulsar wind nebulae. These types of pulsars can have BBPL emissions with no bright optical counterpart. Because X-ray pulsars are important astrophysical objects, further optical and X-ray observations and analysis of the archival data of these sources will be interesting even if they are not magnetars.

It is difficult to determine what the sources with a single-component emission are. These sources are very faint, and their X-ray spectra are not constrained. A spectrum of any faint X-ray source would be fitted to a BB or PL model. Therefore, we did not list them separately. As optical and X-ray survey goes deeper, we should be able to identify them better using our automated package.

Our survey is incomplete because we used only a subset of the archival Chandra data and optical catalogs and because the time resolution of ACIS-I is 3.2 sec, which is insufficient for the detection of a magnetar with a period of less than ~6 sec. Only a small number of observations are obtained with a 0.4 sec time resolution. Moreover, very faint sources were excluded from the search. Further studies of the currently available and future X-ray data will aid in identifying more magnetars and other interesting X-ray sources.

ACKNOWLEDGMENTS

REFERENCES

An H, Hascoët R, Kaspi VM, Beloborodov AM, Dufour F, et al., *NuSTAR* observations of mangetar 1E 1841-045, Astrophys. J. 779, 163 (2013). https://doi.org/10.1088/0004-637X/779/2/163

An H, Kaspi VM, Beloborodov AM, Kouveliotou C, Archibald RF, et al., *NuSTAR* observations of X-ray bursts from the magnetar 1E 1048.1-5937, Astrophys. J. 790, 60 (2014). https://doi.org/10.1088/0004-637X/790/1/60

An H, Archibald RF, Hascoët R, Kaspi VM, Beloborodov AM, et al., Deep *NuSTAR* and *SWIFT* monitoring observations of the magnetar 1E 1841-045, Astrophys. J. 807, 93 (2015). https://doi.org/10.1088/0004-637X/807/1/93

Anders E, Grevesse N, Abundances of the elements: Meteoritic and solar, Geochim. Cosmochim. Acta 53, 197-214 (1989). https://doi.org/10.1016/0016-7037(89)90286-X

Beloborodov AM, On the mechanism of hard X-ray emission from Magnetars, Astrophys. J. 762, 13 (2013). https://doi.org/10.1088/0004-637X/762/1/13

Beloborodov AM, Li X, Magnetar heating, Astrophys. J. 833, 261 (2016). https://doi.org/10.3847/1538-4357/833/2/261

Bernardini F, Israel GL, Stella L, Turolla R, Esposito P, et al., Multi-instrument X-ray monitoring of the January 2009 outburst from the recurrent magnetar candidate 1E 1547.0-5408, Astron. Astrophys. 529, A19 (2011). https://doi.org/10.1051/0004-6361/201016197

Bonazzola S, Gourgoulhon E, Gravitational waves from pulsars: Emission by the magnetic field induced distortion, Astron. Astrophys. 312, 675-690 (1996).

Buccheri R, Bennett K, Bignami GF, Bloemen JBGM, Boriakoff V, et al., Search for pulsed γ-ray emission from radio pulsars in the COS-B data, Astron. Astrophys. 128, 245-251 (1983).

Camero A, Papitto A, Rea N, Viganò D, Pons JA, et al., Quiescent state and outburst evolution of SGR 0501+4516, Mon. Not. R. Astron. Soc. 438, 3291-3298 (2014). https://doi.org/10.1093/mnras/stt2432

Camilo F, Scholz P, Serylak M, Buchner S, Merryfield M, et al., Revival of the Magnetar PSR J1622-4950: Observations with MeerKAT, Parkes, *XMM-Newton*, *Swift*, *Chandra* and *NuSTAR*, Astrophys. J. 856, 180 (2018). https://doi.org/10.3847/1538-4357/aab35a

Campana S, Rea N, Israel GL, Turolla R, Zane S, *Swift* and *Chandra* confirm the intensity-hardness correlation of the AXP 1RXS J170849.0-400910, Astron. Astrophys. 463, 1047-1051 (2007). https://doi.org/10.1051/0004-6361:20065482

Chen G, An H, Kaspi VM, Harrison FA, Madsen KK, et al., *NuSTAR* observations of the young, energetic radio pulsar PSR B1509-58, Astrophys. J. 817, 93 (2016). https://doi.org/10.3847/0004-637X/817/2/93

Dib R, Kaspi VM, Scholz P, Gavriil FP, *RXTE* observations of anomalous X-ray pulsar 1E 1547.0-5408 during and after its 2008 and 2009 outbursts, Astrophys. J. 748, 3 (2012). https://doi.org/10.1088/0004-637X/748/1/3

Esposito P, Mereghetti S, Tiengo A, Zane S, Turolla R, et al., SGR 1806-20 about two years after the giant flare: *Suzaku, XMM-Newton* and *INTEGRAL* observations, Astron. Astrophys. 476, 321-330 (2007). https://doi.org/10.1051/0004-6361:20078562

Esposito P, Tiengo A, Mereghetti S, Israel GL, De Luca A, et al., *XMM-Newton* discovery of 2.6s pulsations in the soft gamma-ray repeater SGR 1627-41, Astrophys. J. Lett. 690, L105-L109 (2009). https://doi.org/10.1088/0004-637X/690/2/L105

Esposito P, Israel GL, Turolla R, Mattana F, Tiengo A, et al., Long-term spectral and timing properties of the soft gamma-ray repeater SGR 1833-0832 and detection of extended X-ray emission around the radio pulsar PSR B1830-08, Mon. Not. R. Astron. Soc. 416, 205-215 (2011). https://doi.org/10.1111/j.1365-2966.2011.19022.x

Evans IN, Primini FA, Glotfelty KJ, Anderson CS, Bonaventura NR, et al., The *Chandra* source catalog, Astrophys. J. Suppl. Ser. 189, 37-82 (2010). https://doi.org/10.1088/0067-0049/189/1/37

Fahlman GG, Gregory PC, An X-ray pulsar in SNR G109.1-1.0, Nature 293, 202-204 (1981). https://doi.org/10.1038/293202a0

Garmire GP, Bautz MW, Ford PG, Nousek JA, Ricker Jr GR, Advanced CCD imaging spectrometer (ACIS) instrument on the Chandra X-ray observatory, Proc. SPIE 4851, 28-44 (2003). https://doi.org/10.1117/12.461599

Gavriil FP, Kaspi VM, Woods PM, Magnetar-like X-ray bursts from an anomalous X-ray pulsar, Nature 419, 142-144 (2002). https://doi.org/10.1038/nature01011

Gotthelf EV, Halpern JP, Buxton M, Bailyn C, Imaging X-ray, optical, and infrared observations of the transient anomalous X-ray pulsar XTE J1810-197, Astrophys. J. 605, 368-377 (2004). https://doi.org/10.1086/382232

Halpern JP, Gotthelf EV, Two magnetar candidates in HESS supernova remnants, Astrophys. J. 710, 941-947 (2010a). https://doi.org/10.1088/0004-637X/710/2/941

Halpern JP, Gotthelf EV, An energetic magnetar in HESS J1713-381/CTB 37B, Astrophys. J. 725, 1384-1391 (2010b). https://doi.org/10.1088/0004-637X/725/1/1384

Harding AK, Pulsar polar cap and slot gap models: Confronting Fermi data, J. Astron. Space Sci. 30, 145-152 (2013). https://doi.org/10.5140/JASS.2013.30.3.145

Isreal GL, Campana S, Dall'Osso S, Muno MP, Cummings J, et al., The post-burst awakening of the anomalous X-ray pulsar in westerlund 1, Astrophys. J. 664, 448-457 (2007). https://doi.org/10.1086/518224

Israel GL, Esposito P, Rea N, Coti Zelati F, Tiengo A, et al., The discovery, monitoring and environment of SGR J1935+2154, Mon. Not. R. Astron. Soc. 457, 3448-3456 (2016). https://doi.org/10.1093/mnras/stw008

Kaspi VM, Archibald RF, Bhalerao V, Dufour F, Gotthelf EV, et al., Timing and flux evolution of the Galactic center magnetar SGR J1745-2900, Astrophys. J. 786, 84 (2014). https://doi.org/10.1088/0004-637X/786/2/84

Kuiper L, Hermsen W, den Hartog PR, Collmar W, Discovery of luminous pulsed hard X-ray emission from anomalous X-ray pulsars 1RXS J1708-4009, 4U0142+61, and 1E 2259+586 by *INTEGRAL* and *RXTE*, Astrophys. J. 645, 556-575 (2006). https://doi.org/10.1086/504317

Mazets EP, Golenetskii SV, Il'inskii VN, Aptekar' RL, Guryan YA, Observations of a flaring pulsar in Dorado, Nature 282, 587-589 (1979). https://doi.org/10.1038/282587a0

Mereghetti S, Esposito P, Tiengo A, Zane S, Turollar R, et al., The first *XMM-Newton* observations of the soft gamma-ray repeater SGR 1900+14, Astrophys. J. 653, 1423 (2006). https://doi.org/10.1086/508682

Mereghetti S, Pons JA, Melatos A, Magnetars: Properties, Origin and Evolution, Space Sci. Rev. 191, 315-338 (2015). https://doi.org/10.1007/s11214-015-0146-y

Muno MP, Clark JS, Crowther PA, Dougherty SM, de Grijs R, et al., A neutron star with a massive progenitor in westerlund 1, Astrophys. J. Lett. 636, L41-L44 (2006). https://doi.org/10.1086/499776

Olausen SA, Kaspi VM, The McGILL magnetar catalog, Astrophys. J. Suppl. Ser. 212, 6 (2014). https://doi.org/10.1088/0067-0049/212/1/6

Rea N, Nichelli, E, Israel GL, Perna R, Oosterbroek T, et al., Very deep X-ray observations of the anomalous X-ray pulsar 4U

0142+614, Mon. Not. R. Astron. Soc. 381, 293-300 (2007). https://doi.org/10.1111/j.1365-2966.2007.12257.x

Rea N, Esposito P, Turolla R, Israel GL, Zane S, et al., A low-magnetic field soft gamma repeater, Science 330, 944-946 (2010). https://doi.org/10.1126/science.1196088

Rea N, Israel GL, Esposito P, Pons JA, Camero-Arranz A, et al., A new low magnetic field magnetar: The 2011 outburst of Swift J1822.3-1606, Astrophys. J. 754, 27 (2012). https://doi.org/10.1088/0004-637X/754/1/27

Rea N, Israel GL, Pons JA, Turolla JA, Viganò D, et al., The outburst decay of the low magnetic field magnetar SGR 0418+5729, Astrophys. J. 770, 65 (2013). https://doi.org/10.1088/0004-637X/770/1/65

Sato T, Bamba A, Nakamura R, Ishida M, Identification of CXOU J171405.7-381031 as a new magnetar with *XMM-Newton*, Publ. Astron. Soc. Jpn. 62, L33-L36 (2010). https://doi.org/10.1093/pasj/62.5.L33

Skrutskie MF, Cutri RM, Stiening R, Weinberg MD, Schneider S, et al., The two micron all sky survey (2MASS), Astron. J. 131, 1163-1183 (2006). https://doi.org/10.1086/498708

Tam CR, Gavriil FP, Dib R, Kaspi VM, Woods PM, et al., X-ray and near-IR variability of the anomalous X-ray pulsar 1E 1048.1-5937: From quiescence back to activity, Astrophys. J. 677, 503-514 (2008). https://doi.org/10.1086/528368

Thompsom C, Duncan RC, The soft gamma repeaters as very strong magnetized neutron stars I. Radiative mechanism for outbursts, Mon. Not. R. Astron. Soc. 275, 255-300 (1995). https://doi.org/10.1093/mnras/275.2.255

Tiengo A, Esposito P, Mereghetti S, *XMM-Newton* observations of CXOU J010043.1-721134: The first deep look at the soft X-ray emission of a magnetar, Astrophys. J. Lett. 680, L133-L136 (2008). https://doi.org/10.1086/590078

Tiengo A, Esposito P, Mereghetti S, Israel GL, Stella L, et al., Quiet but still bright: *XMM-Newton* observations of the soft gamma-ray repeater SGR 0526-66, Mon. Not. R. Astron. Soc. 399, L74-L78 (2009). https://doi.org/10.1111/j.1745-3933.2009.00728.x

Verner DA, Ferland GJ, Korista KT, Yakovlev DG, Atomic data for astrophysics. II. New analytic fits for photoionization cross sections of atoms and ions, Astrophys. J. 465, 487-498 (1996). https://doi.org/10.1086/177435

Wang Y, Takata J, Cheng KS, Mechanism of the X-ray and soft gamma-ray emissions from the high magnetic field pulsar: PSR B1509-58, J. Astron. Space Sci. 30, 91-94 (2013). https://doi.org/10.5140/JASS.2013.30.2.091

Woods PM, Kouveliotou C, Finger MH, Göğüş E, Wilson CA, et al., The prelude to and aftermath of the giant flare of 2004 December 27: persistent and pulsed X-ray properties of SGR 1806-20 from 1993 to 2005, Astrophys. J. 654, 470-486 (2007). https://doi.org/10.1086/507459

Wu JHK, Hui CY, Huang RHH, Kong AKH, Cheng KS, et al., Pulsed γ-ray emission from magnetar 1E 2259+586, J. Astron. Space Sci. 30, 83-85 (2013). https://doi.org/10.5140/JASS.2013.30.2.083

Zacharias N, Monet DG, Levine SE, Urban SE, Gaume R, et al., The Naval Observatory merged astrometric dataset (NOMAD), Bull. American Astron. Soc. 36, 1418 (2004).

Zhu W, Kaspi VM, Dib R, Woods PM, Gavriil FP, et al., The long-term radiative evolution of anomalous X-ray pulsar 1E 2259+586 after its 2002 outburst, Astrophys. J. 686, 520-527 (2008). https://doi.org/10.1086/591219